AFFDL-TR-68-150

ACCURACY AND CONVERGENCE OF FINITE ELEMENT APPROXIMATIONS

Joseph E. Walz, Robert E. Fulton,
and Nancy Jane Cyrus

NASA Langley Research Center
Langley Station, Hampton, Va.

The paper reports on a theoretical investigation of the convergence properties of several finite element approximations in current use and assesses the magnitude of the principal errors resulting from their use for certain classes of structural problems. The method is based on classical order of error analyses commonly used to evaluate finite difference methods. Through the use of the Taylor series differential or partial differential equations are found which represent the convergence and principal error characteristics of the finite element equations. These resulting equations are then compared with known equations governing the continuum, and the error terms are evaluated for selected problems. Finite elements for bar, beam, plane stress, and plate bending problems are studied as well as the use of straight or curved elements to approximate curved beams. The results of the study provide basic information on the effect of interelement compatibility, unequal size elements, discrepancies in triangular element approximations, flat element approximations to curved structures, and the number of elements required for a desired degree of accuracy.

SECTION I

INTRODUCTION

Finite element methods have been used for many years with success in the analysis of complex structures and many aerospace structures are designed on the basis of these analyses. In spite of such widespread use, not enough is known of the theoretical accuracy and convergence properties of these models when used to represent a structure. Accuracy studies are usually based on numerical solutions to restricted problems for comparison with known results. Convergence studies are carried out by investigating the convergence of the numerical results as the number of elements is increased (Reference 1). Such methods, while valuable in providing a cursory assessment of the reliability of various model approximations, are heavily dependent on the numerical data and the problem studied and may obscure the true character of the approximation. More basic information is needed on the theoretical convergence properties of various finite elements for structural approximations.

The purpose of the present paper is to report on a theoretical investigation of the accuracy of several stiffness finite element method approximations in current use and to assess the magnitude of the errors resulting from the use of these approximations for certain classes of structural problems. The present paper documents preliminary results on convergence of several models given orally in Reference 2, extends the study to additional models, and utilizes this data for accuracy investigations. The method used is based on classical order of error analyses commonly used to evaluate the discretization errors of finite difference methods. Through the use of the Taylor series, the ordinary or partial differential equations are found from which the convergence and error characteristics of the finite element equations can be determined. These resulting equations are then compared with the known equations governing the structure. An estimate of the discretization error in the finite element approximation is evaluated by procedures given in References 3 and 4 for a limited class of deflection and vibration problems to provide simple formulas for the size of an element required to obtain a certain degree of accuracy. Finite elements for bar, beam, plane stress, and plate bending problems are studied as well as the use of straight and curved elements to approximate a curved beam.

SECTION II

ERROR ANALYSIS PROCEDURE

Two major sources of error result from the use of finite element methods to solve structural problems. These may be conveniently separated into round-off error and discretization error. Round-off error is that error associated with the accuracy with which numbers are manipulated in a computer and is not considered in the present paper. Discretization error is that error associated with using discrete variables to represent a problem where the state variables are continuous. This error occurs irrespective of the accuracy of numerical calculations and occurs in structural problems when finite elements are used to approximate a continuous structure. Discretization error may be of two kinds: (1) errors proportional to the size of the element which vanish as the element size vanishes and (2) errors which do not vanish when the element size vanishes. Elements and/or patterns which lead to the second kind of discretization errors are unsatisfactory approximations and should be recognized and avoided. The present paper deals with an assessment of discretization error in finite element approximations.

The method used in the study is to obtain the typical finite element equations which express force equilibrium at a reference node point in terms of displacement variables. These finite element equations (which are a class of difference equations) are then expanded in Taylor series about the nodal point to obtain the differential equations equivalent to the finite element equations at that node. The resulting differential equations are compared with the governing equations for the continuum approximated. A simple bar element approximation is treated in detail as an example to characterize the method and to define the terms to be used in the study.

DISCRETIZATION ERRORS

The force-displacement relations of a typical one-dimensional structural element having ends i-1 and i are

$$\begin{bmatrix} F_{i-1} \\ F_i \end{bmatrix} = K \begin{bmatrix} \delta_{i-1} \\ \delta_i \end{bmatrix} \tag{1}$$

where F_i and δ_i are the vector of nodal forces and displacements at the i^{th} node and K is the element stiffness matrix. Consider a bar of constant cross sectional area A subjected

to a distributed axial load p(x) and approximated by finite elements, where x denotes distance along the bar (Figure 1). For a bar finite element F_i is the nodal extensional force, δ_i is the corresponding displacement u_i and

$$K = \frac{EA}{h}\begin{bmatrix} 1 & -1 \\ -1 & 1 \end{bmatrix} \tag{2}$$

where h is the length of the element and E is Young's modulus.

In finite element methods distributed loads are replaced by concentrated loads at the node points. There are several rational ways in which distributed loads may be converted to concentrated loads. The primary purpose of the present paper is to investigate the accuracy of finite element approximations to structures and this can be done by using a very simple lumping procedure for loads. This procedure, for example, for the bar gives the concentrated load as the value of the distributed load at a grid point multiplied by one-half of the total length of the two adjoining elements. Treating the distributed load in this manner and utilizing Equations 1 and 2 leads to the following equation for equilibrium at a typical i^{th} point located between two segments of length h and αh (Figure 1).

$$\frac{EA}{h}\left[-u_{i-1} + u_i\right] + \frac{EA}{\alpha h}\left[u_i - u_{i+1}\right] = \frac{p_i h\,(1+\alpha)}{2} \tag{3}$$

Equation 3 is a typical finite element equilibrium equation for the indicated approximation.

The behavior of the system of Equation 3 is investigated as the number of equations goes to infinity and the size of the element vanishes. This is done by examining Equation 3 in the limit as h approaches zero with the aid of the Taylor series expansion of displacements at points i-1 and i+1 about the i^{th} point. This procedure results in

$$u'' - \frac{h}{3}(1-\alpha)\,u''' + \frac{h^2}{12}\,\frac{(1+\alpha^3)}{1+\alpha}\,u^{iv} + \cdots + \frac{p}{EA} = 0 \tag{4}$$

where primes denote differentiation with respect to x and where the subscript i has been omitted from u_i. (Omission of such subscripts is done consistently throughout the paper). Equation 4 is the differential equation equivalent to the finite element equation at the i^{th} node. The terms in Equation 4 which are not multiplied by powers of h comprise exactly the governing differential equation for the continuous bar and the remaining terms are the discretization errors resulting from use of the finite element approximations.

If a finite element equation converges to the governing differential equation for the continuous structure as h vanishes, the finite element approximation will be defined in this paper to be a consistent approximation. Those terms in Equation 4 which differ from the continuous

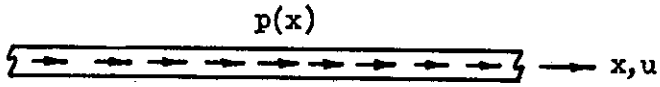

(a) Continuous bar.

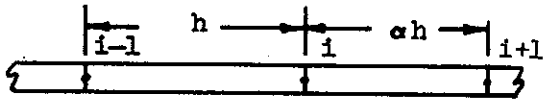

(b) Approximation of continuous bar by finite elements.

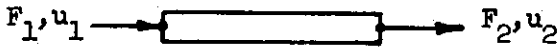

(c) Forces and displacements in bar finite elements.

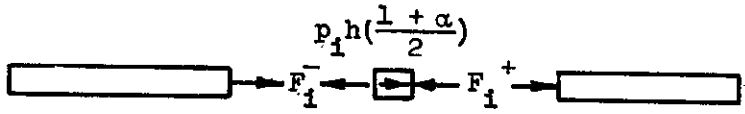

(d) Equilibrium at i^{th} grid point in finite element assemblage.

Figure 1. One Dimensional Bar and Its Finite Element Representation

structure equation are the discretization errors and the principal error in the approximation is the set of terms in the discretization error multiplied by the lowest power of h. The power of h multiplying the principal error denotes the order of the discretization error of the finite element equation and the rate of convergence as h vanishes. Thus, the finite element equation leading to equation (4) has a discretization error of order h. Note that if the segments are equal ($\alpha = 1$), the discretization error is of order h^2. Similarly, if the finite element equations do not converge to the governing differential equations, the discretization error would be of order h^0 or one.

HARMONIC LOADING AND VIBRATION EXAMPLE

The error analysis procedure described in the previous section gives only the rate of convergence of the finite element approximation. The magnitude of the discretization error

in the bar finite element approximation can be evaluated for the special case of a bar supported at each end, subjected to a sinusoidally distributed static loading

$$p = p_o \sin \frac{m\pi x}{L} \tag{5}$$

and approximated by equal length elements. In Equation 5 p_o is the amplitude of the loading, m the number of half waves and L the length of the bar. For this case Equation 4 becomes

$$u'' + \frac{h^2}{12} u^{iv} + \cdots + \frac{p_o}{EA} \sin \frac{m\pi x}{L} = 0 \tag{6}$$

If the loading is regarded as a continuous function as was done in Reference 3 and 4, the solution to Equation 6 is

$$u = u_o \sin \frac{m\pi x}{L} \tag{7}$$

where u_o is the amplitude of the displacement. Substitution of Equation 7 into Equation 6 results in

$$u = \frac{u_{ex}}{1-\epsilon} \approx u_{ex} \left[1+\epsilon\right] \tag{8}$$

where

$$u_{ex} = \frac{p_o}{EA} \left(\frac{L}{m\pi}\right)^2 \sin \frac{m\pi x}{L} \tag{9}$$

is the exact solution to the bar for the sine loading,

$$\epsilon = \frac{\pi^2}{12N^2} \tag{10}$$

is the principal error in deflection resulting due to the finite element approximation and

$$N = \frac{L/m}{h} \tag{11}$$

is the number of elements per harmonic half-wave used to approximate the bar. The following are results for various values of N and error

N	ϵ
3	0.10
4	.05
9	.01

Thus, approximately three elements per deflection half-wave are needed to keep the error in finite element deflection calculations at a node to within ten percent.

A similar approach can be used to determine the error in natural frequency of the bar example when approximated by equal length elements. For vibration behavior where a simple lumping process is used to obtain a diagonal mass matrix the counterpart of Equation 6 is

$$u'' + \frac{h^2}{12} u^{iv} + \cdots \frac{\overline{m}\,\omega^2}{EA} u = 0 \tag{12}$$

where $\overline{m}$ is the mass per unit length and ω is the circular frequency. The vibration mode shape is the same as Equation 7 and the eigenvalues of Equation 12 are

$$\omega^2 = \omega_{ex}^2 \left[1 - \epsilon \right] \tag{13}$$

where

$$\omega_{ex}^2 = \left(\frac{L}{m\pi} \right)^2 \frac{EA}{\overline{m}} \tag{14}$$

and ϵ is the discretization error due to the finite element approximation given by Equation 10. Note that the error in the square of frequency is the same as that resulting from static deflection calculations except of opposite sign. Thus, the frequency calculations converge from below and deflection calculations converge from above.

For completeness, Table I(a) summarizes the principal error terms for the general bar finite element approximations and Table II evaluates these errors for the harmonic response examples.

SECTION III

RESULTS AND DISCUSSION

The method described in the previous section was used to investigate the convergence of beam elements, straight and curved element approximations to an arch, rectangular and triangular plane stress elements, and plate bending elements. The results of the investigation are summarized in this section together with a general discussion. A summary of the error study details is given in Tables I and II.

ONE DIMENSIONAL BENDING ELEMENT

When bending behavior is introduced finite element models and the discretization error analysis procedure become more complex. To indicate the additional features brought on by bending, consider a simple prismatic beam subjected to lateral pressure q and approximated by an assemblage of beam bending finite elements of length h (Figure 2). The finite element nodal variables for this problem are

$$\delta_i = \begin{bmatrix} w_i \\ \theta_i \end{bmatrix} \tag{15}$$

where w_i and θ_i are the displacement and rotation at a node, and two finite element equilibrium equations are obtained at each node. These two equations are expanded in a Taylor series about the i^{th} point (considering both w and θ as independent variables) giving

$$-12w'' - h^2 w^{iv} - \frac{h^4}{30} w^{vi} - \frac{h^6}{1680} w^{viii} + \cdots + 12\theta' + 2h^2 \theta''' + \frac{h^4}{10}\theta^{v} + \frac{h^6}{420}\theta^{viii} + \cdots = \frac{qh^2}{EI} \tag{16}$$

$$\theta = w' + \frac{h^2}{6} w''' + \frac{h^4}{120} w^{v} + \frac{h^6}{5040} w^{vii} + \cdots - \frac{h^2}{6}\theta'' - \frac{h^4}{72}\theta^{iv} - \frac{h^6}{2160}\theta^{vi} + \cdots \tag{17}$$

where I is the moment of inertia of the beam cross section. Since beam behavior for a continuum is defined by only one independent variable w, it is useful to eliminate θ in so far as possible from the finite element equation. This is done by differentiating Equation 17 to obtain expressions for derivatives of θ and sequentially back substituting these derivatives into both Equations 16 and 17.

TABLE I.- FINITE ELEMENT DISCRETIZATION ERROR

(a) One-Dimensional Elements

Element	Nodal variables	Governing differential equations	Error terms (appearing in left-hand side of equations)
BAR (a) Unequal segments	$\{u\}$	$u'' + \frac{p}{EA} = 0$	$-\frac{h}{3}(1-\alpha)\,u''' + \frac{h^2}{12}\frac{(1+\alpha^3)}{(1+\alpha)}\,u^{iv} + \ldots$
(b) Equal segments	"	"	$+\frac{h^2}{12}\,u^{iv} + \ldots$
BEAM	$\begin{Bmatrix} w \\ \theta \end{Bmatrix}$	$w^{iv} = \frac{q}{EI}$ $\theta = w'$	$-\frac{h^4}{720}\,w^{viii} + \ldots$ $+\frac{h^4}{180}\,w^{v} + \ldots$
ARCH (a) Straight segments	$\begin{Bmatrix} u \\ w \\ \theta \end{Bmatrix}$	$EA\left(-u'' + \frac{w'}{R}\right) - p = 0$ $EI\left(w^{iv} + 2\frac{w''}{R^2} + \frac{w}{R^4}\right) + EA\left(-\frac{u'}{R} + \frac{w}{R^2}\right) - q = 0$ $\theta = w' + \frac{u}{R}$	$-\frac{EI}{R}\left(w''' + \frac{u''}{R}\right) + O(h^2)$ $-\frac{EI}{R}\left(\frac{w}{R^3} + \frac{2w''}{R} - u'''\right) + O(h^2)$ $+ O(h^2)$
(b) Curved segments	"	" " "	$+ O(h^2)$ $+ O(h^2)$ $+ O(h^2)$

TABLE I.- FINITE ELEMENT DISCRETIZATION ERROR - Continued

(b) Plane Stress Elements

Variables $\begin{Bmatrix} u \\ v \end{Bmatrix}$

Governing differential equations

(1) $u_{,xx} + \frac{1-\mu}{2} u_{,yy} + \frac{1+\mu}{2} v_{,xy} + \frac{p_x}{B} = 0$

(2) $\frac{1+\mu}{2} u_{,xy} + \frac{1-\mu}{2} v_{,xx} + v_{,yy} + \frac{p_y}{B} = 0$

Element	Equation number	Error terms (appearing in left-hand side of equations)
Rectangle, linear stress distribution	(1)	$+ \frac{h^2}{12}\left\{u_{,xxxx} + \left[\frac{3}{2}(1-\mu) + \alpha^2(2+\mu^2)\right]u_{,xxyy} + \frac{1-\mu}{2}\alpha^2 u_{,yyyy} + (1+\mu)v_{,xxxy} + (1+\mu)\alpha^2 v_{,xyyy}\right\} + \cdots$
	(2)	$+ \frac{h^2}{12}\left\{(1+\mu)u_{,xxxy} + (1+\mu)\alpha^2 u_{,xyyy} + \frac{1-\mu}{2} v_{,xxxx} + \left[\frac{3}{2}\alpha^2(1-\mu) + (2+\mu^2)\right]v_{,xxyy} + \alpha^2 v_{,yyyy}\right\} + \cdots$
Rectangle, linear edge displacement	(1)	$+ \frac{h^2}{12}\left\{u_{,xxxx} + \left[(1-\mu) + 2\alpha^2\right]u_{,xxyy} + \frac{1-\mu}{2}\alpha^2 u_{,yyyy} + (1+\mu)v_{,xxxy} + (1+\mu)\alpha^2 v_{,xyyy}\right\} + \cdots$
	(2)	$+ \frac{h^2}{12}\left\{(1+\mu)u_{,xxxy} + (1+\mu)\alpha^2 u_{,xyyy} + \frac{1-\mu}{2} v_{,xxxx} + \left[\alpha^2(1-\mu) + 2\right]v_{,xxyy} + \alpha^2 v_{,yyyy}\right\} + \cdots$
Right triangle, Pattern A	(1)	$+ \frac{h^2}{12}\left[u_{,xxxx} + \alpha^2\left(\frac{1-\mu}{2}\right)u_{,yyyy} + 2\alpha\, v_{,xxxy} + 3\alpha^2 v_{,xxyy} + 2\alpha^3 v_{,xyyy}\right] + \cdots$
	(2)	$+ \frac{h^2}{12}\left[2\alpha\, u_{,xxxy} + 3\alpha^2 u_{,xxyy} + 2\alpha^3 u_{,xyyy} + \left(\frac{1-\mu}{2}\right) v_{,xxxx} + \alpha^2 v_{,yyyy}\right] + \cdots$
Right triangle, Pattern B	(1)	$- \frac{1+\mu}{2} v_{,xy} + \frac{h^2}{12}\left[u_{,xxxx} + \frac{1-\mu}{2}\alpha^2 u_{,yyyy}\right] + \cdots$
	(2)	$- \frac{1+\mu}{2} u_{,xy} + \frac{h^2}{12}\left[\frac{1-\mu}{2} v_{,xxxx} + \alpha^2 v_{,yyyy}\right] + \cdots$
Right triangle, Pattern C	(1)	$+ \frac{1+\mu}{2} v_{,xy} + \frac{h^2}{12}\left[u_{,xxxx} + \frac{1-\mu}{2}\alpha^2 u_{,yyyy} + 2(1+\mu)\, v_{,xxxy} + 2(1+\mu)\alpha^2 v_{,xyyy}\right] + \cdots$
	(2)	$+ \frac{1+\mu}{2} u_{,xy} + \frac{h^2}{12}\left[2(1+\mu)u_{,xxxy} + 2(1+\mu)\alpha^2 u_{,xyyy} + \frac{1-\mu}{2} v_{,xxxx} + \alpha^2 v_{,yyyy}\right] + \cdots$
Equilateral triangle	(1)	$+ h^2\left[\frac{7+\mu}{96} u_{,xxxx} + \frac{1+\mu}{16} u_{,xxyy} + \frac{1-\mu}{32} u_{,yyyy} + \frac{1+\mu}{48} v_{,xxxy} + \frac{1+\mu}{16} v_{,xyyy}\right] + \cdots$
	(2)	$+ h^2\left[\frac{1+\mu}{16} u_{,xxxy} + \frac{1+\mu}{48} u_{,xyyy} + \frac{1-\mu}{32} v_{,xxxx} + \frac{1+\mu}{16} v_{,xxyy} + \frac{7+\mu}{96} v_{,yyyy}\right] + \cdots$

TABLE I.- FINITE ELEMENT DISCRETIZATION ERROR - Concluded

(c) Rectangular Plate Bending Elements

Variables $\begin{Bmatrix} w \\ \theta \\ \varphi \end{Bmatrix}$

Governing differential equations

(1) $\nabla^4 w = \frac{q}{D}$

(2) $\theta = w_{,x}$

(3) $\varphi = w_{,y}$

Element	Equation number	Error terms (appearing in left-hand side of equations)
Melosh	(1)	$+ h^2\left\{\left[\frac{1}{6} - \frac{\mu}{12} + \frac{\alpha^2\mu^2}{48}\right]w_{,xxxxyy} + \left[\alpha^2\left(\frac{1}{6} - \frac{\mu}{12}\right) + \frac{\mu^2}{48}\right]w_{,xxyyyy}\right\} + \ldots$
	(2)	$+ O(h^2)$
	(3)	$+ O(h^2)$
ACM	(1)	$+ h^2\left[\frac{1}{6}\left(\alpha^2 + \mu\right)w_{,xxxxyy} + \frac{1}{6}\left(1 + \mu\alpha^2\right)w_{,xxyyyy}\right] + \ldots$
	(2)	$+ O(h^4)$
	(3)	$+ O(h^4)$
Papenfuss	(1)	$+ \left(\frac{2}{35}\alpha^2 + \frac{2}{35\alpha^2} + \frac{2}{25}\right)w_{,xxyy} + h^2\left[\left(\frac{\alpha^6}{3675} + \frac{2}{2625}\alpha^4 + \frac{274}{91875}\alpha^2 - \frac{61}{2625} - \frac{146}{3675\alpha^2}\right)w_{,xxxxyy} + \alpha^2\left(\frac{1}{3675\alpha^6} + \frac{2}{2625\alpha^4} + \frac{274}{91875\alpha^2} - \frac{61}{2625} - \frac{146\alpha^2}{3675}\right)w_{,xxyyyy}\right] + \ldots$
	(2)	$+ O(h^2)$
	(3)	$+ O(h^2)$

TABLE II.- ERROR TERMS FOR HARMONIC RESPONSE EXAMPLES

Element	Error terms
Bar $p = p_o \sin \frac{m\pi x}{L}$ $u = u_{ex}(1 + \epsilon)$ $u_{ex} = \frac{p_o}{EA}\left(\frac{L}{m\pi}\right)^2 \sin \frac{m\pi x}{L}$ $\omega^2 = \omega_{ex}^2 (1 - \epsilon)$ $\omega_{ex}^2 = \frac{EA}{\bar{m}}\left(\frac{m\pi}{L}\right)^2$	$\epsilon = \frac{\pi^2}{12N^2} \qquad \left(N = \frac{L}{mh}\right)$
Beam $q = q_o \sin \frac{m\pi x}{L}$ $w = w_{ex}(1 + \epsilon)$ $w_{ex} = \frac{q_o}{EI}\left(\frac{L}{m\pi}\right)^4 \sin \frac{m\pi x}{L}$ $\omega^2 = \omega_{ex}^2 (1 - \epsilon)$ $\omega_{ex}^2 = \frac{EI}{\bar{m}}\left(\frac{m\pi}{L}\right)^4$	$\epsilon = \frac{\pi^4}{720N^4}$
Arch $p = 0$ $q = q_o \sin \frac{mx}{R}$ $u = u_{ex}(1 + \epsilon_u)$ $w = w_{ex}(1 + \epsilon_w)$ $u_{ex} = \frac{-q_o R^4}{EIm\left(m^2 - 1\right)^2} \cos \frac{mx}{R}$ $w_{ex} = \frac{q_o R^4}{EI\left(m^2 - 1\right)^2} \sin \frac{mx}{R}$	(a) Straight segments $\epsilon_u = m^2\left(\frac{\rho}{R}\right)^2 + O(h^2)$ $\epsilon_w = \left(\frac{\rho}{R}\right)^2 + O(h^2)$ (b) Curved segments $\epsilon_u = O(h^2)$ $\epsilon_w = O(h^2)$

TABLE II.- ERROR TERMS FOR HARMONIC RESPONSE EXAMPLES - Concluded

Element	Error terms
Plane stress rectangle $p_x = 0$ $p_y = p_o \sin \frac{m\pi x}{a} \sin \frac{n\pi y}{a}$ $u = u_{ex}(1 + \epsilon_u)$ $v = v_{ex}(1 + \epsilon_v)$ $u_{ex} = \frac{p_o a^2 (1+\mu) mn}{B\pi^2 (1-\mu)\left(m^2+n^2\right)^2} \cos \frac{m\pi x}{a} \cos \frac{n\pi y}{a}$ $v_{ex} = \frac{2p_o a^2 \left(m^2 + \frac{1-\mu}{2} n^2\right)}{B\pi^2 (1-\mu)\left(m^2+n^2\right)^2} \sin \frac{m\pi x}{a} \sin \frac{n\pi y}{a}$	(a) Linear stress distribution $\epsilon_u = \frac{h^2\pi^2 m^2 n^2 (5 - 2\mu + \mu^2)}{12a^2(m^2+n^2)}$ $\epsilon_v = \frac{h^2\pi^2}{6a^2(1-\mu)} \left\{ \frac{1-\mu}{2} m^8 + \frac{13 - 16\mu + 3\mu^2}{4} m^6 n^2 + \frac{16 - 26\mu + 11\mu^2 - 2\mu^3 + \mu^4}{4} m^4 n^4 + \frac{6 - 14\mu + 9\mu^2 - 2\mu^3 + \mu^4}{4} m^2 n^6 + \left(\frac{1-\mu}{2}\right)^2 n^8 \right\} \Big/ \left[m^6 + \frac{5-\mu}{2} m^4 n^2 + (2-\mu) m^2 n^4 + \frac{1-\mu}{2} n^6 \right]$ (b) Linear edge displacement $\epsilon_u = \frac{h^2\pi^2 m^2 n^2 (7 - 10\mu - \mu^2)}{24a^2(m^2+n^2)(1-\mu)}$ $\epsilon_v = \frac{h^2\pi^2}{6a^2(1-\mu)} \left\{ \frac{1-\mu}{2} m^8 + \frac{11 - 14\mu - \mu^2}{4} m^6 n^2 + \frac{27 - 45\mu + 9\mu^2 + \mu^3}{8} m^4 n^4 + \frac{11 - 25\mu + 13\mu^2 + \mu^3}{8} m^2 n^6 + \left(\frac{1-\mu}{2}\right)^2 n^8 \right\} \Big/ \left[m^6 + \frac{5-\mu}{2} m^4 n^2 + (2-\mu) m^2 n^4 + \frac{1-\mu}{2} n^6 \right]$
Rectangular plate $q = q_o \sin \frac{m\pi x}{a} \sin \frac{n\pi y}{a}$ $w = w_{ex}(1 + \epsilon_1)$ $w_{ex} = \frac{q_o a^4}{D\pi^4 \left[m^2+n^2\right]^2} \sin \frac{m\pi x}{a} \sin \frac{n\pi y}{a}$ $\omega^2 = \omega_{ex}^2 (1 - \epsilon_2)$ $\omega_{ex}^2 = \frac{D\pi^4 \left(m^2+n^2\right)^2}{\bar{m} a^4}$	(a) Melosh $\epsilon_1 = \epsilon_2 = \frac{h^2\pi^2}{a^2} \left(\frac{1}{6} - \frac{\mu}{12} + \frac{\mu^2}{48}\right) \frac{m^2 n^2}{(m^2+n^2)}$ (b) ACM $\epsilon_1 = \epsilon_2 = \frac{h^2\pi^2}{a^2} \left(\frac{1+\mu}{6}\right) \frac{m^2 n^2}{(m^2+n^2)}$ (c) Papenfuss $\epsilon_1 = \frac{-m^2 n^2}{\left(m^2+n^2\right)^2 + \frac{34}{175} m^2 n^2} \left\{ \frac{34}{175} + \frac{h^2\pi^2 (5416)\left(m^2+n^2\right)^3}{a^2 (91875) \left[\left(m^2+n^2\right)^2 + \frac{34}{175} m^2 n^2\right]} \right\}$ $\epsilon_2 = \frac{-m^2 n^2}{(m^2+n^2)} \left[\frac{34}{175(m^2+n^2)} + \frac{h^2\pi^2 (5416)}{a^2 (91875)} \right]$

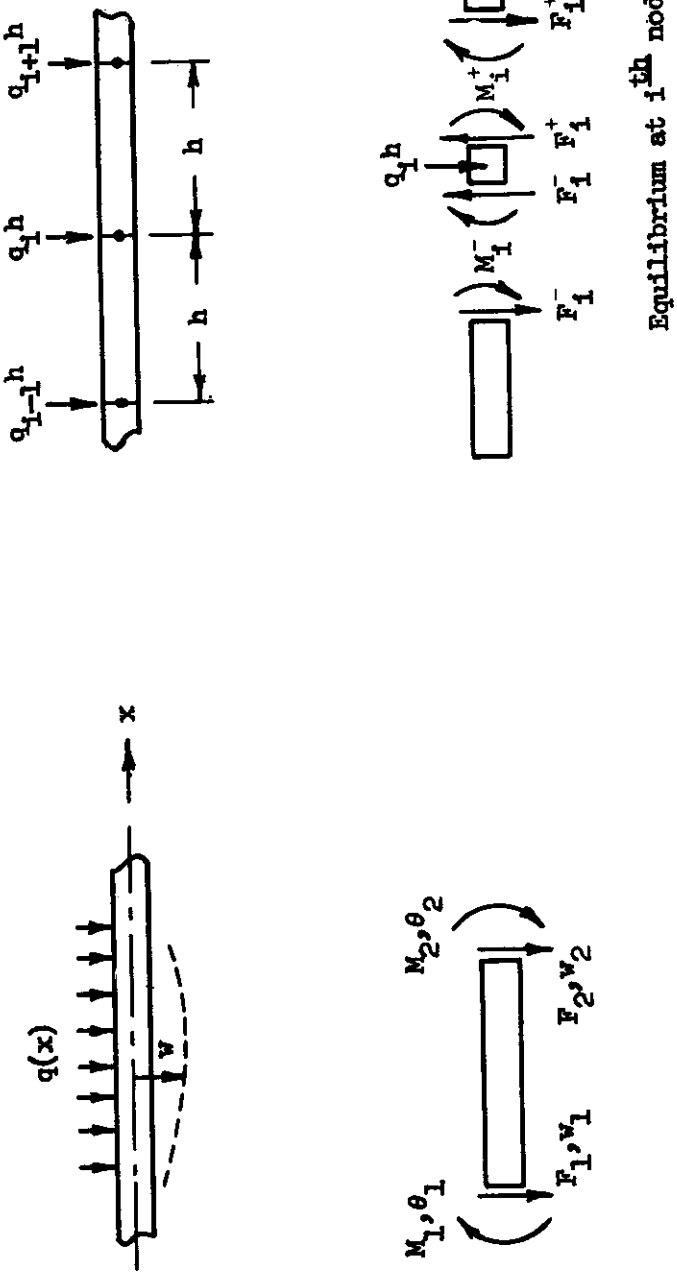

Figure 2. Beam Element

Equations 16 and 17 finally can be put in the form

$$w^{iv} - \frac{h^4}{720} w^{viii} + \cdots = \frac{q}{EI} \tag{18}$$

$$\theta - w' + \frac{h^4}{180} w^{v} + \cdots = 0 \tag{19}$$

Equations 18 and 19 show that in the limit as h vanishes the beam finite element equations converge to the familiar beam equation and the correct constraint equation between the two finite element variables θ and w. The equations also show that the principal error term in the approximation is order h^4 (Table I(a)).

The principal error was evaluated for a finite element approximation to a simply supported beam of length L subjected to a sinusoidally distributed lateral load q.

$$q = q_o \sin \frac{m\pi x}{L} \tag{20}$$

where q_o is a constant. The error in the lateral deflection w of the beam due to the finite element approximation is (Table II).

$$\epsilon = \frac{\pi^4}{720N^4} \tag{21}$$

Equation 21 also gives the magnitude of the error in frequency determination due to the finite element approximation (Table II).

APPROXIMATION OF CURVED STRUCTURES

Straight elements are often being used to approximate curved structures such as curved beams, arches, and shells. To gain some insight into the influence of curvature, an arch of radius R was approximated by conventional straight beam elements which also had extensional capability. The arch loading is a normal pressure q and a tangential distributed loading p (Figure 3). At a typical i^{th} node three variables are required to define element behavior. For this problem it is convenient to take these variables as

$$\delta_i = \begin{bmatrix} u_i \\ w_i \\ \theta_i \end{bmatrix} \tag{22}$$

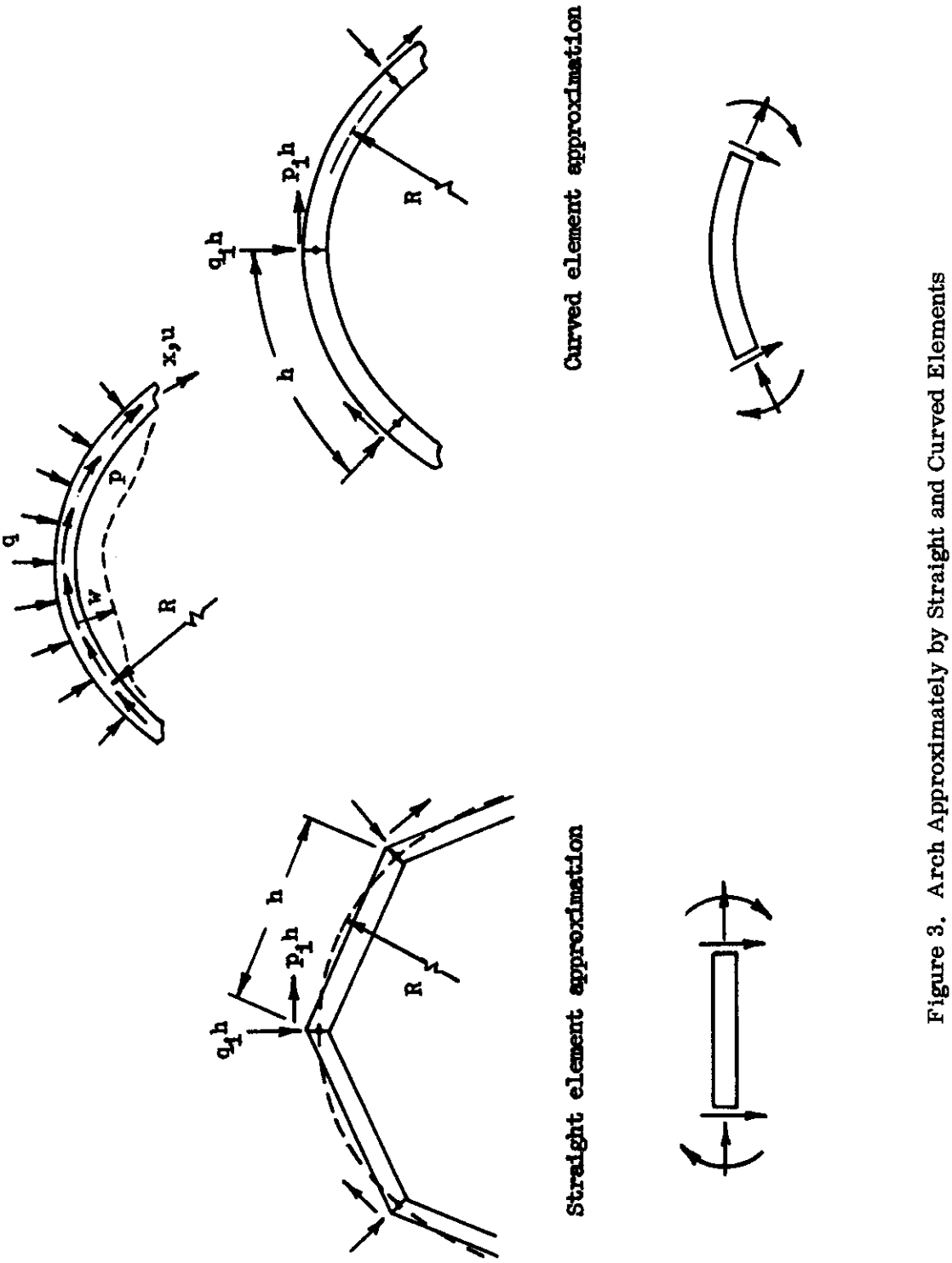

Figure 3. Arch Approximately by Straight and Curved Elements

where u and w are the tangential and radial displacements and θ the rotation. Three finite element equations result from force and moment equilibrium. As the element size vanishes, the moment equilibrium equation at the i^{th} node converges to the correct constraint equation between the rotation θ, radial displacement w, and tangential displacement u

$$\theta - \left(w' + \frac{u}{R} \right) = 0 \tag{23}$$

and the tangential and normal equilibrium equations converge, respectively, to

$$EA \left(-u'' + \frac{w'}{R} \right) - p = \frac{EI}{R} \left(w''' + \frac{u''}{R} \right) \tag{24}$$

$$EI \left(w^{iv} + 2 \frac{w''}{R^2} + \frac{w}{R^4} \right) + EA \left(\frac{-u'}{R} + \frac{w}{R^2} \right) - q = \frac{EI}{R} \left(\frac{w}{R^3} + \frac{2w''}{R} - u''' \right) \tag{25}$$

In Equations 24 and 25 the rotation θ has been eliminated by using Equation 23 in a manner similar to that done earlier for the other bending problems. A typical set of arch continuum equations such as those given in Reference 5 is composed of only the left-hand side of Equations 23, 24, and 25; namely, equation 23 plus

$$EA \left(-u'' + \frac{w'}{R} \right) - p = 0 \tag{26}$$

$$EI \left(w^{iv} + 2 \frac{w''}{R^2} + \frac{w}{R^4} \right) + EA \left(- \frac{u'}{R} + \frac{w}{R^2} \right) - q = 0 \tag{27}$$

Comparison of Equations 24 and 25 with 26 and 27 shows that finite element equations resulting from a straight element approximation do not converge to these arch equations since the right side of 24 and 25 does not vanish. Thus, the discretization error appears to be of order one and suggests that some errors result from the use of straight elements to approximate the bending behavior of the curved structure.

A study was also made of the use of curved elements to approximate the curved structure. While the details have been omitted here the stiffness matrix for a curved element was derived from the strain energy consistent with arch Equations 26 and 27 (Reference 5). The displacements were approximated by assuming that arch tangential and normal displacements, were linear and cubic, respectively, over the curved element length. The resulting finite element equations were investigated and it was found that the element pattern converged to the arch Equations 26 and 27 with an error of order h^2.

An assessment of the magnitude of the order one discretization error terms in Equations 24 and 25 can be obtained by considering a closed circular ring subjected to a harmonic lateral loading and approximated by straight elements. In the limit as the element size h vanishes the resulting straight element psuedo arch is governed by Equations 24 and 25 and

$$p = 0 \tag{28}$$

$$q = q_o \sin \frac{mx}{R} \tag{29}$$

The principal errors in the u and w deflections ϵ_u and ϵ_w due to the finite element approximation are (Table II)

$$\epsilon_u = m^2 \left(\frac{\rho}{R} \right)^2 \tag{30}$$

$$\epsilon_w = \left(\frac{\rho}{R} \right)^2 \tag{31}$$

where ρ is the radius of gyration of the arch. Equations 28 through 31 indicate that the order one discretization errors lead to errors in deflection which are proportional to the square of the ratio of the radius of gyration to the arch radius. For a typical arch cross section these errors are quite small and well within accuracy requirements for engineering purposes provided enough elements are used. Tangential displacement errors are also proportional to m^2; however, the ring theory breaks down for very high harmonics.

Since the magnitude of the order one errors are proportional to $\left(\frac{\rho}{R}\right)^2$ and therefore quite small for thin arches it suggests that Equations 24 and 25 are acceptable arch equations. Further investigation shows that a suitable thin arch theory can, in fact, be derived which leads to Equations 24 and 25. This theory can be obtained from the arch theory of Reference 5 if the change in curvature are modified by an additional term which is the extensional strain divided by the arch radius.* According to the Koiter criteria for thin shells (Reference 12) such modifications are admissible variations of a first approximation theory of thin shells and it seems reasonable to apply this criteria to arch theory. Thus both straight and curved elements provide a convergent approximation to a first approximation thin arch theory as the element size vanishes.

*The authors are indebted to Professor B. Budiansky of Harvard University for suggesting that alternate first approximation arch theories be investigated.

TWO DIMENSIONAL PLANE STRESS ELEMENTS

The linear elastic plane stress equations for equilibrium in the x and y directions formulated in terms of displacements are, respectively:

$$u_{,xx} + \frac{1-\mu}{2} u_{,yy} + \frac{1+\mu}{2} v_{,xy} + \frac{p_x}{B} = 0 \tag{32}$$

$$\frac{1+\mu}{2} u_{,xy} + \frac{1-\mu}{2} v_{,xx} + v_{,yy} + \frac{p_y}{B} = 0 \tag{33}$$

Here u and v are the displacements in the x and y directions, respectively, p_x, p_y the distributed forces, μ Poisson's ratio, $B = Et/\left(1-\mu^2\right)$ the extensional stiffness and t the plate thickness. A satisfactory finite element approximation should lead to equations which converge to Equations 32 and 33 at a node as the element size vanishes.

Rectangular Elements

Two rectangular plane stress plate elements were investigated in the study and their stiffness properties are documented in reference 6. For the first model, denoted linear stress model, the stresses in the x and y directions are assumed to vary linearly while the shear stress is constant (Figure 4). For the second model, denoted a linear edge displacement model, the displacements along an edge of the element are assumed to vary linearly. The nodal variables used to define the stiffness matrices for these finite elements are

$$\delta_i = \begin{bmatrix} u_i \\ v_i \end{bmatrix}$$

and a typical finite element equation contains contributions from all elements contiguous to the node. The pattern arrangement composed of equal elements is shown in Figure 4. The distributed forces on the plane stress body were again concentrated in a simple fashion based on the value of the distributed force at each node location. The typical finite element equations were obtained and the error terms evaluated. An investigation of the convergence of the finite element equilibrium equation for both models showed them to converge to the plane stress equations 32 and 33 with a principal error of order h^2. (Table I(b)).

The principal error was evaluated for the case where the two rectangular elements were used to approximate a square plate in plane stress subjected to a harmonic in-plane loading, in the y direction. The loading is

$$p_x = 0 \tag{34}$$

$$p_y = p_o \sin \frac{m\pi x}{a} \sin \frac{n\pi y}{a} \tag{35}$$

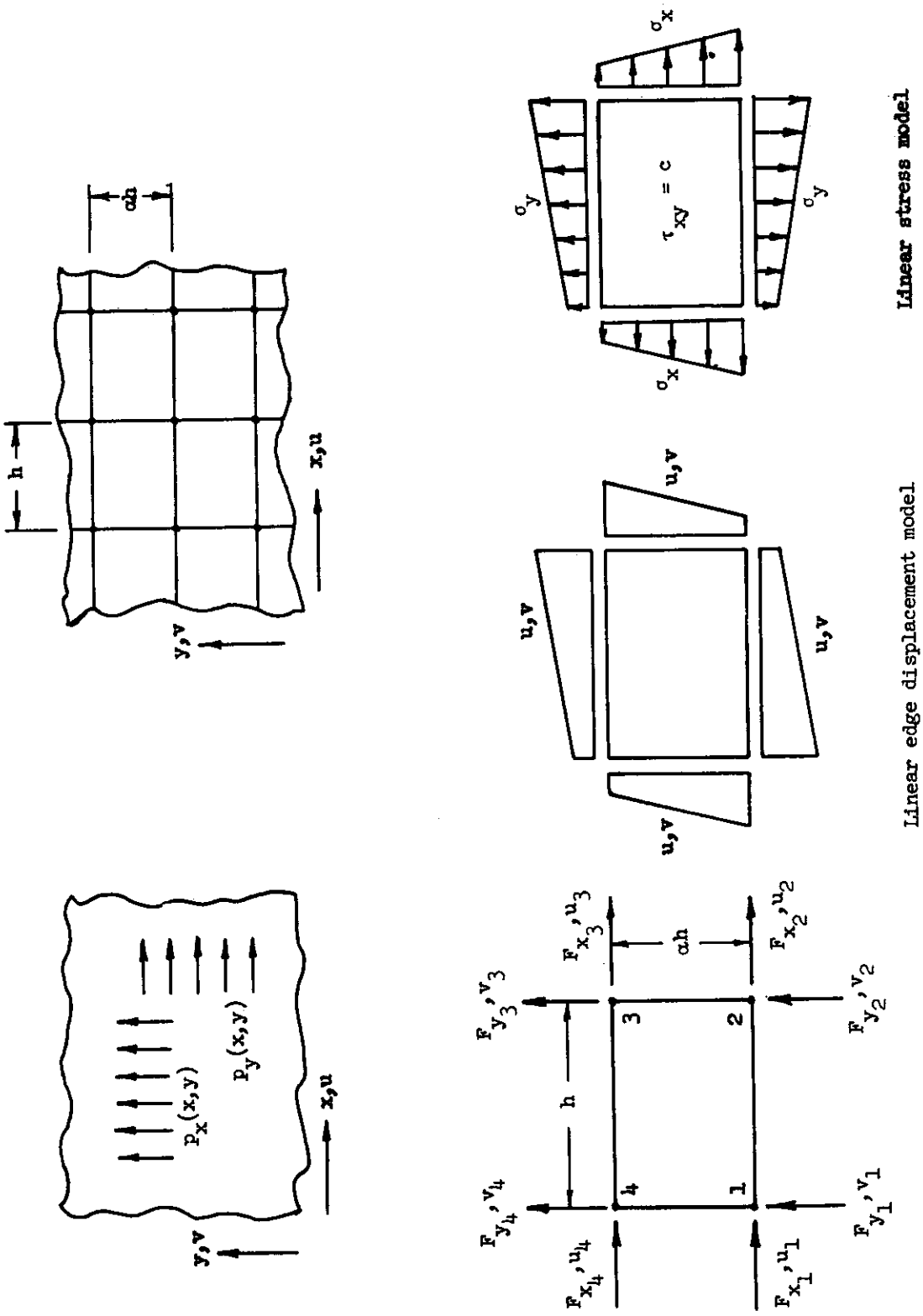

Figure 4. Plane Stress Element

and the plate is supported on the boundary such that the force resultant in the x direction and the v displacement both vanish. For $\mu = 0.3$ and m = n the errors in the u and v displacements, ϵ_u and ϵ_v, respectively, are (Table II).

1. linear stress model

$$\epsilon_u = \frac{1.85}{N^2} \tag{36}$$

$$\epsilon_v = \frac{2.40}{N^2} \tag{37}$$

2. linear edge displacement model

$$\epsilon_u = \frac{1.15}{N^2} \tag{38}$$

$$\epsilon_v = \frac{1.97}{N^2} \tag{39}$$

where N is the number of elements per half wave-length.

Triangular Elements

Results were also obtained for the use of the classical triangular plate element (Reference 7) to approximate plane stress problems. Arrangements or patterns A, B, and C were investigated for the convergence of three right triangular elements (Figure 5 for patterns about ij point). It was found that pattern A converges to the required plane stress equations 32 and 33 and the principal error is of order h^2. On the other hand, the corresponding equations for pattern B are

$$u_{,xx} + \frac{1-\mu}{2} u_{,yy} + \frac{p_x}{B} = 0 \tag{40}$$

$$\frac{1-\mu}{2} v_{,xx} + v_{,yy} + \frac{p_y}{B} = 0 \tag{41}$$

and pattern C are

$$u_{,xx} + \frac{1-\mu}{2} u_{,yy} + (1+\mu) v_{,xy} + \frac{p_x}{B} = 0 \tag{42}$$

$$(1+\mu) u_{,xy} + \frac{1-\mu}{2} v_{,xx} + v_{,yy} + \frac{p_y}{B} = 0 \tag{43}$$

The additional error terms for all patterns proportional to h^2 are given in Table I(b).

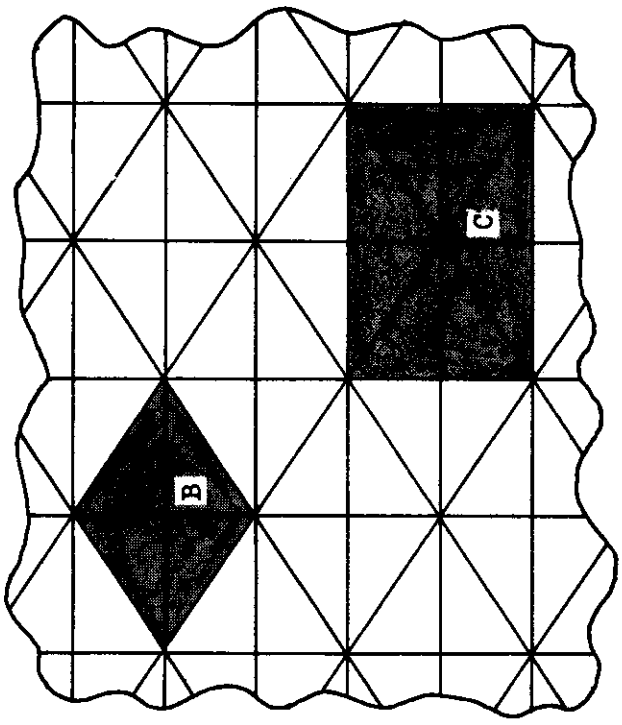

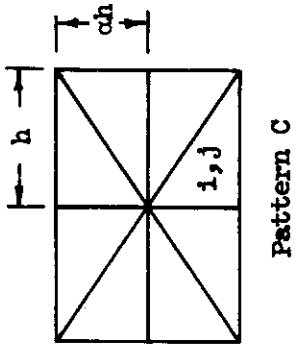

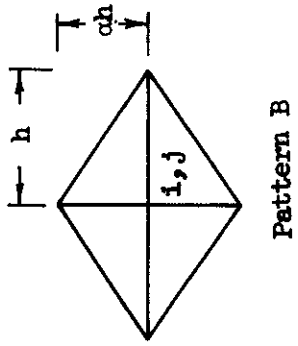

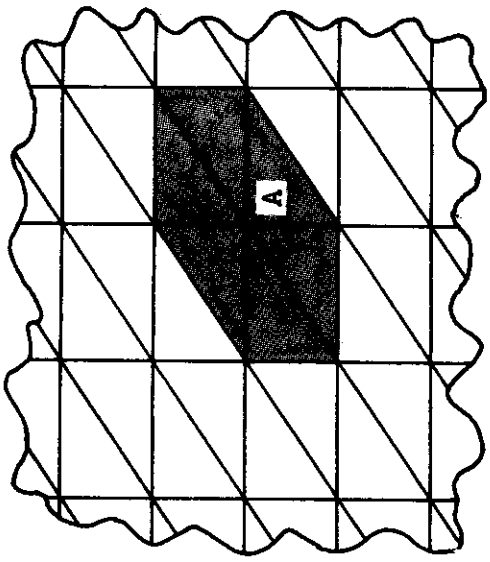

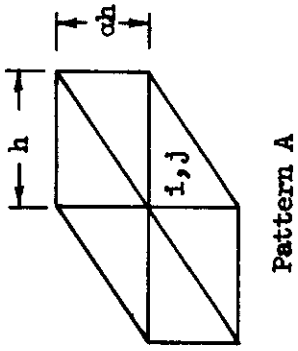

Figure 5. Triangular Finite Element Patterns

Some points can be noted by comparing the convergence characteristics when h = 0 of the B and C equations with Equations 32 and 33. First of all both patterns B and C lead to a discretization error of order one. The pattern B equations do not contain cross-derivative terms suggesting that convergence of shear behavior at the nodal point is poor. This is not unexpected since there is no mechanism in the finite element equations for representing changes in shear at the nodal point due to the arrangement of the elements. On the other hand, the pattern C equations over prescribe the cross-derivative term by a factor of two. Note that the difficulty arises from the element arrangement rather than the element properties since the element used here fully represents all states of plane stress. This indicates that convergence difficulties may arise for some triangular elements as a result of poor element arrangement even though the element is well formulated.

Since the difficulty with pattern B is due to its inability to represent the cross derivative at the node, better convergence properties would be expected if additional degrees of freedom were used to characterize the right triangular element behavior. Such added degrees of freedom might be the deflections at the midpoint of the various edges or the derivatives of displacements at nodes.

Fortunately, if patterns B and C are used in structural idealizations, they usually occur in pairs (Figure 5) and the under prediction of the shear stiffness at one point is compensated for to some extent by an over prediction of shear stiffness at a neighboring point. Nevertheless, these results do suggest that caution should be exercised to ensure that an excessive number of either patterns A or B does not occur in a structure when the results are strongly dependent on shear stiffness. A more consistent approach is to use pattern A since it converges to the appropriate plane stress equation.

For completeness, the convergence of a pattern composed of equilateral triangles in plane stress was also investigated. The typical pattern is shown in Figure 6 and the resulting finite element equations were found to converge to the plane stress equations with a principal error of order h^2. (Table I(b)).

TWO-DIMENSIONAL PLATE BENDING ELEMENTS

Three rectangular plate bending models were investigated to determine the convergence and principal errors of the resulting finite element equations. The models investigated were those developed by Papenfuss (Reference 8), Melosh (Reference 9), and one developed

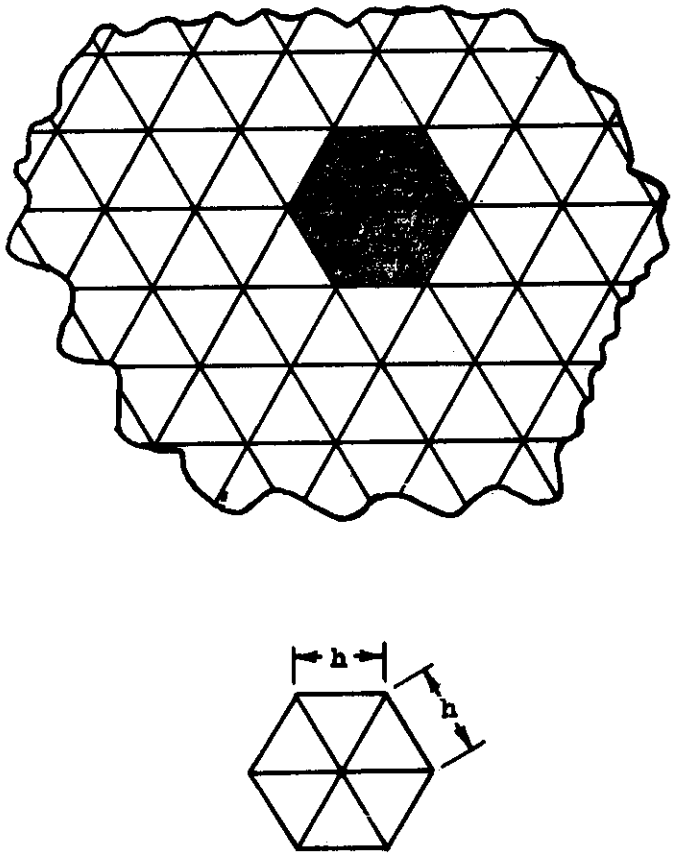

Figure 6. Equilateral Triangular Finite Element Pattern

independently by Adini and Clough (Reference 1 or Reference 10) and Melosh (Reference 11). (These will be denoted respectively as the Papenfuss, Melosh, and ACM models.) The pattern arrangement is shown in Figure 7. The nodal variables for these finite element models are

$$\delta_i = \begin{bmatrix} w_i \\ \theta_i \\ \phi_i \end{bmatrix} \tag{44}$$

where w is the lateral displacement and θ and ϕ the rotations about the y and x axes, respectively. On the basis of the beam results a consistent set of three plate bending finite element equations should be expected to converge to

$$\nabla^4 w = \frac{q}{D} \tag{45}$$

$$\theta = w_{,x} \tag{46}$$

$$\phi = w_{,y} \tag{47}$$

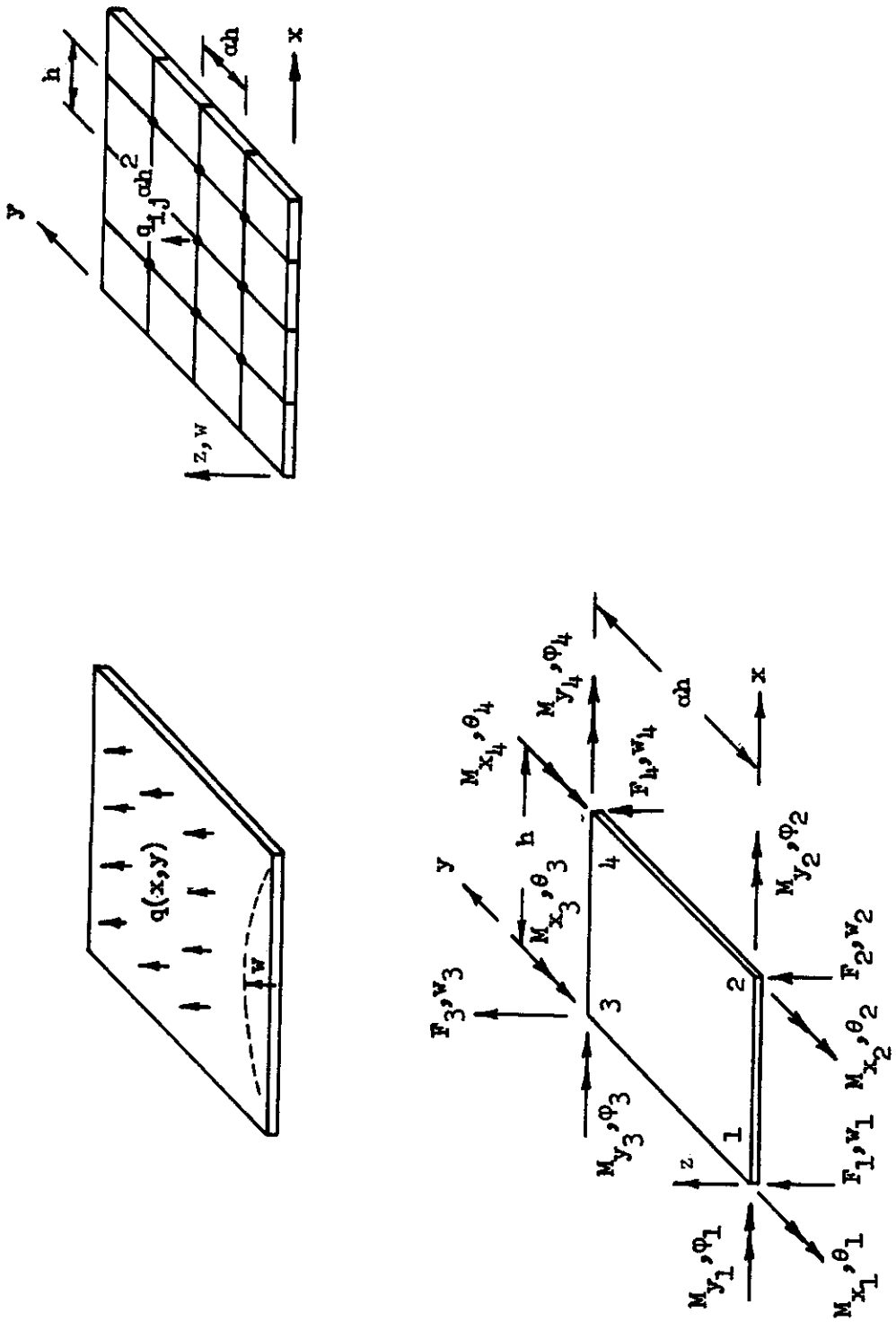

Figure 7. Plate Bending Element

as the element size vanishes. Here Equation 45 is the familiar plate equation and Equations 46 and 47 are constraint equations between the rotations θ and ϕ and derivative of w. The finite element equilibrium equations for the three models at a node point were expanded in a Taylor series and manipulated to a convenient form in a manner similar to that done for the beam equations. All three models lead to equations which converge to constaint equations of the form of Equations 46 and 47 and the Melosh and ACM models also converge to the Plate Equation 45. The Papenfuss model, however, converges to a psuedo plate equation

$$\nabla^4 w + \left(\frac{2\alpha^2}{35} + \frac{2}{35\alpha^2} + \frac{2}{25}\right) w_{,xxyy} = \frac{q}{D} \tag{48}$$

where α is the aspect ratio of the element and thus has a principal error of order one. The principal errors for all other equations for the three models are proportional to h^2 with the exception of the constraint equations for the ACM model which are proportional to h^4 (Table I(c)).

It is well known from numerical calculations (Reference 1) that the Papenfuss model has some deficiencies and that the source of the discrepancies is the inability of the model to describe the twist behavior of a plate. This discrepancy term shows up as an incorrect cross-derivative term in Equation 48 when h vanishes.

Square elements of the three models were then used to approximate a simply supported square plate subjected to a harmonic loading.

$$q = q_0 \sin \frac{m\pi x}{a} \sin \frac{n\pi x}{a} \tag{49}$$

The same procedure was used to approximate the lateral vibration characteristics of the plate. The error in deflection ϵ_1 and the error in frequency ϵ_2 due to the finite element approximation is, for m = n and $\mu = 0.3$ (Table II).

	Papenfuss	Melosh	ACM
ϵ_1	$-.0463 - \frac{.2646}{N^2}$	$\frac{.708}{N^2}$	$\frac{1.069}{N^2}$
ϵ_2	$-.0486 - \frac{.2909}{N^2}$	$\frac{.708}{N^2}$	$\frac{1.069}{N^2}$

where $N = \frac{a/m}{h}$ is the number of elements per Fourier half-wave. Figure 8 shows a sketch of the plate and a plot of the ratio of the finite element results to the exact result for the three elements as the $1/N^2$ vanishes. The results show that in the limit as the size of the element vanishes, the results for this problem based on the Papenfuss model have an error of approximately five percent. Note also that the Papenfuss model converges from below and the other two models converge from above.

Since the Papenfuss model equations do not converge to the plate equation, a solution was obtained for the resulting Papenfuss psuedo plate Equation 48 for a rectangular planform subjected to a uniform load $\bar{q}$, having simple support boundary conditions and approximated by elements having the same aspect ratio as the plate. The solution was obtained by classical Fourier series expansion for the load $\bar{q}$ and deflection shape as

$$\bar{q} = \sum_{m=1} \sum_{n=1} q_{mn} \sin \frac{m\pi x}{a} \sin \frac{n\pi y}{b} \tag{50}$$

$$w = \sum_{m=1} \sum_{n=1} w_{mn} \sin \frac{m\pi x}{a} \sin \frac{n\pi y}{b} \tag{51}$$

where a and b are the lengths of the plate in the x and y direction, respectively.

The w_{mn} are related to the $\bar{q}$ by

$$w_{mn} = \frac{16\,\bar{q}}{\pi^2 D\, mn \left[\frac{m^4}{a^4} + \frac{m^2 n^2}{a^2 b^2}\left(2 + \frac{2a^2}{35} + \frac{2}{35a^2} + \frac{2}{25}\right) + \frac{n^4}{b^4}\right]}$$

The following compares the center deflection w_c of the Papenfuss psuedo plate with the exact plate results

$$\frac{w_c D}{\bar{q} a^4} \times 10^3$$

	Papenfuss Plate	Exact
a/b = 1	3.87	4.06
a/b = 1/2	9.64	10.13

These results indicate that the Papenfuss psuedo plate has an error of approximately five percent for both cases. Numerical results obtained in Reference 1 for the above cases appear to be converging toward these analytical results.

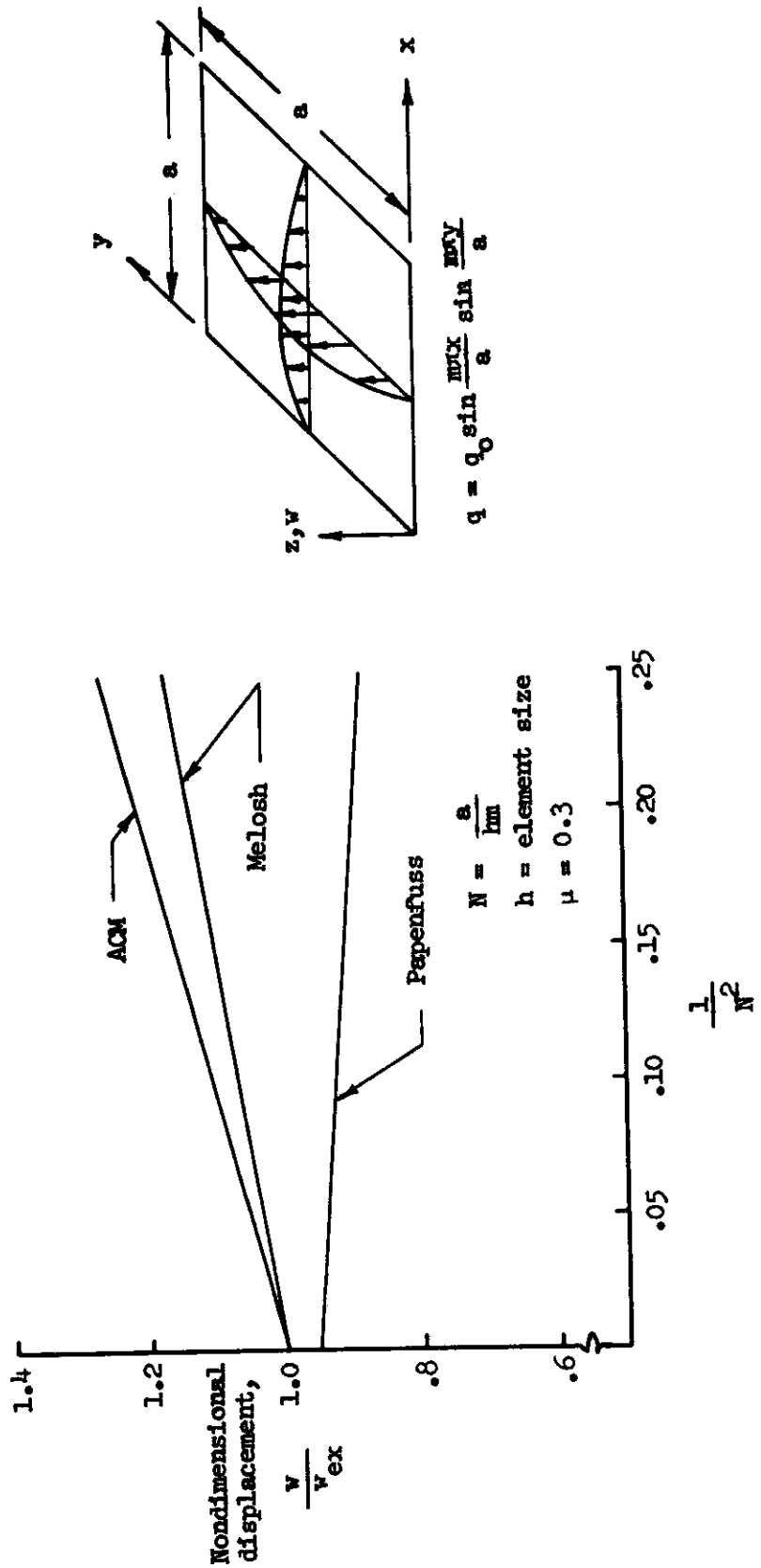

Figure 8. Effect of Grid Size on Displacement of Plate Under Sinusoidally Distributed Loading q

COMPARISON OF ELEMENT MODELS

Some general results can be deduced by comparing the convergence and principal error results of the various element approximations. One result deals with the requirement of interelement compatability. Consideration of the elements for both plane stress and bending gave examples where this requirement was neither necessary nor sufficient to insure convergence. The rectangular linear stress model is not interelement compatible in displacements and the rectangular Melosh and ACM bending models are not compatible in slope; yet these three lead to convergent equations. On the other hand, the right triangular plane stress patterns A and B are interelement compatible in displacements and the Papenfuss plate bending element is compatible in slope and displacements and yet these elements and arrangements do not lead to convergent equations.

Some influence of unequal length segments is seen from the change in principal errors for the bar approximations. For bar elements of equal length the principal error is proportional to h^2 and for bars of unequal length proportional to h. From the asymmetric character of the Taylor series expansion about the reference point similar reduction of the order of error would be expected for other elements. This slower rate of convergence suggests that results may be less accurate when structures are approximated by unequal elements than where approximated by equal length segments.

Comparison of the errors for the plane stress with those of the bar subjected to harmonic loading indicates that approximately nine bar elements and 15 square plane stress elements per half wave in one direction are required for one percent error. Approximately two beam elements and nine square Melosh plate bending elements are required for 1 percent error. This result indicates that more elements are required per wave length in one direction for two-dimensional behavior than for one-dimensional behavior to obtain the same degree of accuracy. This is important because practical complex structures such as stiffened plates or shells are two-dimensional and usually approximated by various combinations of one- and two-dimensional elements. Since the elements have varying degrees of accuracy, results obtained for a structure approximated by a combination of the elements may be biased in some sense rather than having uniform inaccuracies.

SECTION IV

CONCLUDING REMARKS

Basic data are presented on the convergence and accuracy of finite element equations resulting from patterns and elements in common use. The elements studied include bar elements, beam elements, plane stress elements of rectangular and triangular shape, plate bending elements of rectangular shape and straight and curved arch elements. The results indicate that many of the elements and patterns have good convergence properties; that is, the resulting finite element equations at a node converge to the continuum equations at the node as the element size vanishes. The results also indicate that some elements and/or patterns have poor convergence properties. Right triangular plane stress patterns for example, can have undesirable convergence properties. It is shown that the requirement for interelement compatibility is neither necessary nor sufficient to guarantee convergence of the finite element equations. Results for arch approximations show that both straight and curved elements provide a convergent approximation to an arch structure.

SECTION V

REFERENCES

1. Clough, R. W., and Tocher, J. L., "Finite Element Stiffness Matrices for Analysis of Plate Bending." Proceedings of Conference on Matrix Methods in Structural Mechanics. AFFDL-TR-66-80, 1965.

2. Fulton, Robert E., Eppink, Richard T., and Walz, Joseph E., "The Accuracy of Finite Element Methods in Continuum Problems." Presented at the Fifth U. S. National Congress of Applied Mechanics, Minneapolis, Minnesota. June 14-17, 1966.

3. Cyrus, Nancy Jane, and Fulton, Robert E., "Finite Difference Accuracy in Structural Analysis." Proc. ASCE, Journal Struct. Div., Vol. 92, No. 576, pp. 459-471, December 1966.

4. Cyrus, Nancy Jane, and Fulton, Robert E., Accuracy of Finite Difference Methods, NASA TN D-4372, January 1968.

5. Langhaar, H. L., Energy Methods in Applied Mechanics, John Wiley and Sons, Inc., 1962.

6. Gallagher, R. H., A Correlation Study of Methods of Matrix Structural Analysis, AGARograph 69, The Macmillan Company, New York, 1964.

7. Turner, M. J., Clough, R. W., Martin, H. C., and Topp, L. J., "Stiffness and Deflection Analysis of Complex Structures." Journal of Aero. Sci., Vol. 23, No. 9, September 1956, pp. 805-823, 854.

8. Papenfuss, S. W., Lateral Plate Deflection by Stiffness Matrix Methods With Application to a Marquee. M. S. Thesis, Department of Civil Engineering, University of Washington, December 1959.

9. Melosh, R. J., "A Stiffness Matrix for the Analysis of Thin Plates in Bending." Journal Aero Sci., Vol. 28, No. 1, 1961, pp. 34-42, 64.

10. Adini, A, and Clough, R. W., Analysis of Plate Bending by the Finite Element Method. Report submitted to NSF, Grant G-7337, 1960.

11. Melosh, R. J., "Basis for Derivation of Matrices for the Direct Stiffness Method." AIAA Journal, Vol. 1, No. 7, pp. 1631-1637, 1963.

12. Koiter, W. T., "A Consistent First Approximation in the General Theory of Thin Elastic Shells." Proceedings of the Symposium on the Theory of Thin Elastic Shells, North-Holland Publishing Co., Amsterdam, 1960.

SYMBOLS

A	cross-sectional area of one dimensional element
a, b	length of rectangular panel in x and y directions, respectively
B	extensional stiffness of plate, $\frac{Et}{1-\mu^2}$
D	bending stiffness of plate $\frac{Et^3}{12(1-\mu^2)}$
E	Young's modulus
F	finite element nodal force
F_x, F_y	nodal force in x and y directions of plane stress element
h	reference length of finite element
I	moment of inertia of cross section
K	element stiffness matrix
L	length of one dimensional structure
m, n	harmonic wave numbers for sinusoidally distributed loads
$\bar{m}$	mass per unit length for one dimensional element; mass per unit area for two dimensional element
$N = \frac{a}{hm} = \frac{L}{hm}$	number of elements per harmonic wave number
$O(h)$	omitted discretization error term of order h
p	tangential loading on bar and arch structures
p_o	amplitude of sinusoidal in-plane loading
p_x, p_y	distributed in-plane loading in x and y directions
q	transverse loading
q_o	amplitude of sinusoidally distributed transverse loading
R	radius of arch
t	thickness of plate
u, v, w	displacements in x, y and z directions
u_o, v_o, w_o	amplitude of sinusoidally varying displacements
x, y	rectangular coordinates

SYMBOLS (CONT)

α	constant indicating ratio of element dimensions
$\{\delta\}$	vector of nodal displacements
ϵ	discretization error in displacement or frequency parameter
ϵ_u, ϵ_v	discretization error in u and v displacements
θ, ϕ	nodal rotation variables for bending element about y and x axes
μ	Poisson's ratio
ρ	radius of gyration of cross section
ω	circular frequency

SUBSCRIPTS

ex	exact
i	identification for i^{th} grid point